On the Fracture Toughness of Irradiated F82H: Effects of Loss of Constraint and Strain Hardening Capacity – T. Yamamoto, G.R. Odette(University of California Santa Barbara) and M.A. Sokolov (Oak Ridge National Laboratory).

OBJECTIVE

Objective of the research is to examine effects of loss of both constraint and strain hardening capacity on the fracture toughness of irradiated H82H. We have applied a constraint-loss (CL) size effect adjustment procedure to K_{Jm} for F82H-IEA heat irradiated in HFIR to≈ 6.6 dpa at ≈ 300 ºC. We c ompare the ΔT_{mo} based on the SV adjusted measured toughness to the corresponding ΔT_{co} using a physically based size adjustment procedure. We also compare the ΔT_{co} data trends to hardening model predictions. Finally we evaluate the limitations of using the small bend bars used in the High Flux Isotope Reactor (HFIR) irradiations to evaluate static ΔT_{co} for irradiated TMS with loss of strain hardening.

SUMMARY

Constraint loss adjustments, based on finite element (FE) stress analysis and local critical stress, σ^*, critical stressed volume, V*, cleavage criteria were applied to fracture toughness data from small pre-cracked bend bars of the IEA heat of F82H irradiated to 6.6 dpa at 300 ºC in the High Flux Isotope Reactor. The 100 MPa√m master curve method reference temperature shifts were evaluated based on both the measured toughness (ΔT_{mo}) and after size-adjusting the toughness to small scale yielding conditions at reference specimen size (ΔT_o) with values of≈ 148 and 205ºC, respectively. The prediction $\Delta T_o = C_o \Delta\langle\sigma_{fl}\rangle$, where C_o≈ 0.68 and $\Delta\langle\sigma_{fl}\rangle$ is the change in the average flow stress over 0-10% strain is in excellent agreement with ΔT_o. The FE analyses also demonstrate an upper-bound K_{Jc} that can be measured with these small bend bars for irradiated alloys that suffer severe loss of strain hardening.

RESEARCH PROGRESS AND STATUS

Introduction

Irradiation embrittelement, as characterized by upward shifts (ΔT_o) in the cleavage fracture toughness master curve (MC)[1-5], is one of the key issues that control operation window of the 8-9Cr-1-2W normalized and tempered martensitic steels (TMS) in fusion reactor first wall application. At irradiation temperatures less than≈ 400°C, the ΔT_o are primarily due to irradiation hardening, $\Delta\sigma_y$[1,6,7]. However, the weakening of grain boundaries by very high levels of helium may also interact synergistically with large $\Delta\sigma_y$, resulting in very large ΔT_o[1,7,8].

Assessment of irradiation-induced increases in the MC reference temperatures, ΔT_o, requires use of small specimens due to both limited space and high heating rates in available irradiation facilities. However, the fracture toughness measured using small specimens, K_{Jm}, is generally higher than those obtained from larger, conventional specimens, due to both statistical and constraint loss size effects [1,3,5,9]. Statistical effects are related to crack tip stressed volume (SV), where cleavage fracture initiates, scaling with the crack front length (B) as $K_{Jr}=[K_{Jc}(B)-K_{min}][B_r/B]^{1/4}+K_{min}$; here B_r=25.4mm is a reference length and K_{min} = 20MPa√m is a minimum toughness [4,9]. For standard test specimen geometries, the constraint loss (CL) effect is related to the specimen ligament dimension that defines the limit of a embedded plastic region/ligament size ratio that maintains small scale yielding amplitudes of the high blunting crack tip stress fields. CL is significantly enhanced by reduced strain hardening in irradiated steels [1,10] and direct use of measured irradiated K_{Jm} can lead a highly non-conservative ΔT_m unless size effects are correctly accounted for [3,9,11]. Rathbun et al. have shown that physically based models can be used to adjust K_{Jm} data to full constraint reference conditions (plane strain, small scale yielding for B=25.4mm) K_{Jr} [3,5,9,11]. For example, application of the adjustment procedure to a large unirradiated database for F82H, K_{Jm} obtained from 13 types of specimens, resulted in a self-consistent population of K_{Jr} data well described by a single MC with a T_o≈ -103 ± 3 ºC [3].

In the irradiation hardening dominated regime, $\Delta T_o \approx C_o \Delta\sigma_y$, where experimental estimates of C_o range from ≈ 0.7 °C/MPa for reactor pressure vessel (RPV) steels for low dose (< 0.1 dpa) irradiations at $T_i \approx$ 300 °C to as low as ≈ 0.33 °C/MPa for 9Cr tempered martensitic steels (TMS) for irradiations at lower temperatures (e.g., 300°C) irradiations to several dpa [1,10,12-14]. For example Odette et al. reported a $C_o \approx$ 0.58 °C/MPa for F82H irradiated between ≈ 250 to 380°C [1,13] and Sokolov has suggested even lower values [12,14]. It was also shown that the lower C_o for TMS alloys and irradiation conditions, which can be attributed to large reduction of strain hardening [1,10,13]. A model based study by Odette et al. showed that ΔT_o is controlled by a the change in the flow stress averaged over 0 to 10% plastic strain $\Delta\langle\sigma_{fl}\rangle$, that accounts for loss of strain hardening, as $\Delta T_o = 0.68\Delta\langle\sigma_{fl}\rangle$ [10]. He et al. showed theoretically as well as experimentally that the averaged flow stress can be directly related to hardness measurement [15]. As is demonstrated by Yamamoto et al. [6,16], based on the analyses of a large database on $\Delta\sigma_y$ and Chapry DBTT shift, ΔT_c, in irradiated TMS, these hardening-shift relations can be extended to include synergistic interactions with non-hardening embrittlement due to grain boundary weakening accompanying helium accumulation. It was shown that a semi-empirical hardening model for $\Delta\sigma_y(dpa,T_i,T_t)$, where T_i is the irradiation temperature and T_t is the test temperature could be combined with hardening-shift coefficients for Charpy (C_c) tests to predict $\Delta T_c = C_c\Delta\sigma_y(dpa,T_i, He)$.

In this study, we applied a CL size effect adjustment procedure to K_{Jm} for F82H-IEA heat irradiated in HFIR to ≈ 6.6 dpa at ≈ 300 ºC. The primary objectives were to:

- Compare the ΔT_{mo} based on the SV adjusted measured toughness to the corresponding ΔT_{co} using a physically based size adjustment procedure.
- Compare the ΔT_{co} data trends to hardening model predictions.
- Evaluate the limitations of using the small bend bars (see below) used in the High Flux Isotope Reactor (HFIR) irradiations to evaluate static ΔT_{co} for irradiated TMS with loss of strain hardening.

Experimental

Fracture toughness of the irradiated F82H-IEA heat was measured using a pre-cracked bend bar (PCBB) with dimensions of W=3.33, B=1.67 and L=18mm irradiated to nominally 6.6 dpa at 300ºC in the JP-26 capsule in HFIR. Details are reported by Sokolov et al. in ref [14]. Companion miniature tensile specimens, with gauge section of W=1.2, t=0.5 and L=5 mm, were also irradiated in the same capsule nominally to 7.7 dpa at 300 ºC and tested at RT. Details of the tensile test is reported in ref [17].

Constitutive model

Figure 1a shows stress strain curves for the irradiated and unirradiated F82H-IEA heat. The irradiated engineering stress-strain curve, s(e) (blue dashed curve), shows a σ_y = 953MPa and $\Delta\sigma_y$ = 402MPa. Yielding in the irradiated case is followed by immediate necking, hence, the true stress strain curve, $\sigma(\varepsilon)$, could be directly evaluated only up to ≈ 0.4% plastic strain as shown by the solid blue curve. Hence, the $\sigma(\varepsilon)$ required for the crack tip stress field analysis was obtained by iterative FE simulation by modifying trail s(e) input functions until they reproduced the s(e) curves [18,19]. The green dotted (irradiated) and blue curves (unirradiated) in Figure 1b show the final iterated $\sigma(\varepsilon)$ and corresponding predicted engineering stress-strain curves, respectively. The strain hardening was assumed to be independent of temperature and the temperature dependence of σ_y determined from a master curve of thermally activated flow [20].

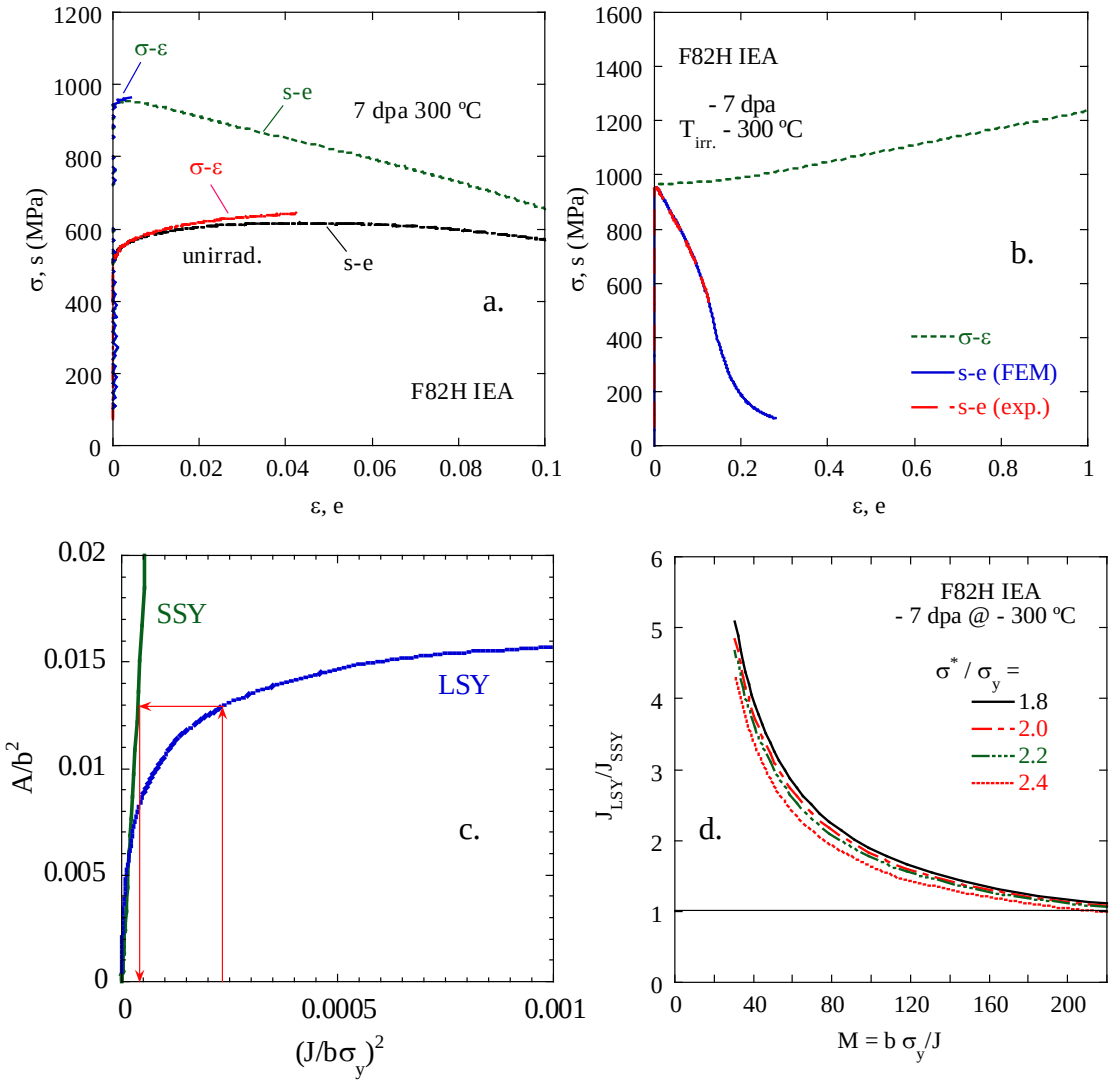

Figure 1 a) Engineering and true stress-strain curves of F82H-IEA before and after neutron irradiation to ≈ 7.7dpa at 300 ºC in HFIR; b) FEM simulated and experimental engineering stress-strain curves (s-e) with an input of constitutive model (s-e) of the irradiated F82H-IEA; c) The normalized stressed area for σ^*/σ_y = 2.0 as a function of $J/b\sigma_y$ for both SSY and LSY conditions showing constraint loss (CL) at higher loading in LSY. Red arrows illustrate the CL adjustment procedure; d) the CL adjustment factor (J_{LSY}/J_{SSY}) as a function of constraint parameter M (= $b\sigma_y/J_{LSY}$) for various σ^*/σ_y ratios.

Size effect adjustment based on FE

Cleavage fracture initiates in the high stress region near the tip of a blunting crack [1,9]. The crack tip fields can be described by isostress contours that reach peak values of 3 to 5 times σ_y, depending on the alloy strain-hardening rate [1,9,22]. Under plane strain, small-scale yielding (SSY) conditions for specimens with a/W≠ 0.5, the spatial dimensions of the stress field scale with the crack tip opening displacement, $\delta \approx J/2\sigma_y$ (or $K_J^2/2\sigma_y E$), where J, K_J, E are J-integral, plastic elastic loading and elastic modulus, respectively[1,9,22]. However, if the deformation level, hence the d, that is required to produce cleavage is not very small compared to the characteristic dimension of the specimen, typically taken as the uncracked ligament length, b = W - a, then the crack tip stress fields fall below small scale yielding values. The reduction of the stress fields at higher $J/b\sigma_y=2\delta/b$ is known as constraint loss (CL) [1,9,22].

Finite element (FE) simulations were performed to obtain the average stressed areas (A) along the crack front as a function of normalized stress σ_{22}/σ_y perpendicular to the crack plane and $J/b\sigma_y$ for the $\sigma(\varepsilon)$ derived previously. Three-dimensional (3D) large scale yielding (LSY) FE models were used to simulate the actual specimen geometry and a 2D plain strain model was used to calculate the fields for small scale yielding (SSY)[1,3,9].

Figure 1c shows normalized A/b^2 versus $[J/b\sigma_y]$ under both SSY and LSY conditions at -40 ºC. for σ^*/σ_y = 2.0. Here it is assumed that σ^* = 2100MPa is unaffected by irradiation and that the calibration value derived from the unirradiated $K_{Jc}(T)$ curve can be used in all cases [3]. Deviation from the linear SSY relation indicates that CL begins at $(J/b\sigma_y)^2 \approx 3\times10^{-5}$ (or $d/b \approx 0.005$) and becomes significant at $(J/b\sigma_y)^2 \approx 5\times10^{-5}$ (or $\delta/b \approx 0.01$). These low deformation are exaggerated by the low σ^*/σ_y ratio ($\approx$ 2.0) at the test temperature and the low strain hardening in irradiated TMS. The red arrows in Figure 1c illustrate a procedure to adjust a toughness value to remove the CL effect. The $(J_{LSY}/b\sigma_y)^2$ value at cleavage for LSY condition is converted to an SSY $(J_{SSY}/b\sigma_y)^2$ for the same A/b^2. The J_{LSY}/J_{SSY} adjustment as a function of $M = b\sigma_y/J_{LSY}$ for various σ^*/σ_y ratios is shown in Figure 1d. The CL begins at M < 200 and is massive at M = 30 which is the very non-conservative constraint loss limit recommended in ASTM E1921 MC method.

Statistical stressed volume (SV) size adjustment relates to the variations in the probability of initiating weakest link cleavage as a function of the total volume (V) of material under high stress. Since for SSY conditions, A scales with J^2 or K_J^4, and $V^*=BA^*$, simple theory suggests that K_{Jc} scales as $\approx B^{-1/4}$ [1,8]. However, other mechanistic considerations and empirical observations show that this $B^{-1/4}$-scaling is modified by a minimum toughness, K_{min}, as $K_{Jr}(B_r)=[K_{Jc}(B)-K_{min}][B_r/B]^{1/4}+K_{min}$ [1,5,8]. The ASTM MC standard E1921, specifies a $K_{min}\approx$ 20 MPa$\sqrt{m}$ and a reference thickness B_r=25.4mm [4]. More detailed description on the CL and SSV size effects adjustment procedures can be found in the literature [1,9,11].

Results and Discussion

Figure 2a shows toughness data of the irradiated PCBB specimens adjusted to a reference B_r = 25.4mm, with (unfilled red squares) and without (blue diamonds) CL-adjustment. Multi-temperature MC analyses [2,4] yields corresponding reference temperatures of T_{coi} = 102 ºC (red lines) and T_{mo} = 39 ºC (blue lines). Note the thick lines are for the median toughness and the thin lines represent the 5% to 95% bounds. The unirradiated MC with $T_{co}\approx$ -103ºC results in shifts of 205 and 247 ºC, with and without CL-adjustment, respectively.

Figure 2b shows ΔT_o as a function of $\Delta\sigma_y$ literature data for irradiations at a similar temperature using relatively large specimens or with CL-adjustments applied [5,13,23,24]. The $\Delta T_o/\Delta\sigma_y$ ratio of 0.51 °C/MPa found in this study falls slightly below the overall fitted trend of $\approx$ 0.56 °C/ MPa. Odette et al. showed that the micromechanical cleavage fracture model used in this study also predicts a universal relation between ΔT_o and the change in the average flow stress $\langle\sigma_{fl}\rangle$ between 0 and 10% plastic strain [10] that accounts for the strain hardening loss in highly irradiated steels. Figure 2c shows the predicted $\Delta T_o(\Delta\langle\sigma_{fl}\rangle)$ relation for various combinations of yield and strain hardening contributions to the overall flow stress, representing the competing effects of irradiation. The $\Delta T_o/\Delta\langle\sigma_{fl}\rangle$ of 0.68 found in this study is a remarkable agreement with the model.

We can also estimate ΔT_o based on the hardening-shift relation $\Delta T_o = C_o\Delta\sigma_y(dpa,T_i)$, where the $\Delta\sigma_y(dpa,T_i)$ was derived from our analysis of the larger TMS database [6]. For T_i = 300 °C, using the $\sigma_y(dpa,T_i)$ model and the C_o = 0.56 °C/MPa for room temperature tensile tests from the fit shown in Figure 2b, yields the relation; $\Delta T_o=286[1- \exp(-dpa/7.7)]^{1/2}$. As shown in Figure 2d, the hardening-shift model $\Delta T_o(dpa)$ predictions are in excellent agreement with experimental data for $T_i\approx$ 300 ºC.

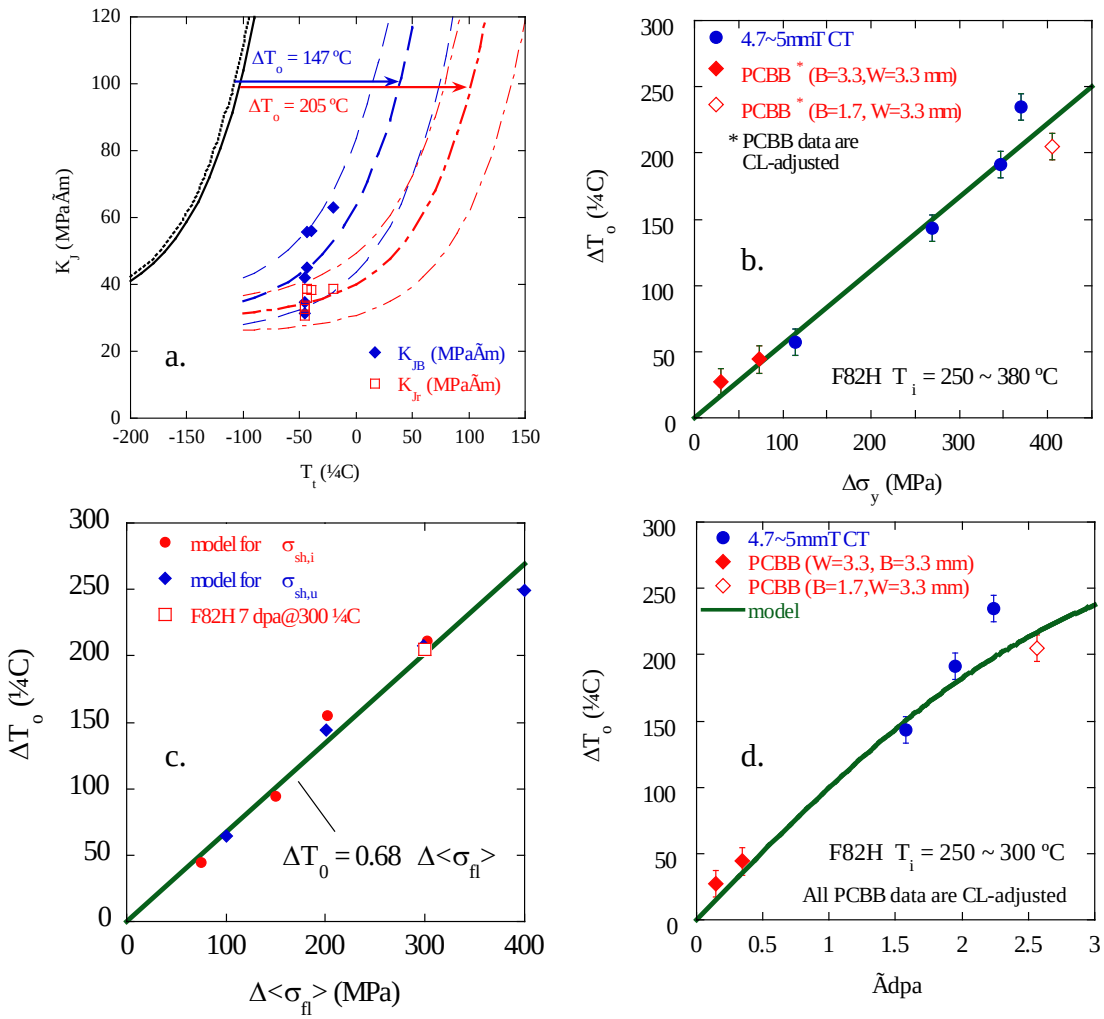

Figure 2 a) 1T-conveted toughness data with MCs before (K_{JB}) and after (K_{Jr}) constraint loss adjustment; b) ΔT_o versus $\Delta\sigma_y$ relations in CL-adjusted PCBB or CT specimens of F82H-IEA irradiated at 250 to 380 ºC to various doses; c) ΔT_o versus $\Delta\langle\sigma_{fl}\rangle$ (change in flow stress) relations of the irradiated F82H compared with theoretical study by Odette et al.[10]. d) ΔT_o in relatively high constraint specimens of F82H irradiated at ≈ 300ºC with irradiation hardening based model prediction.

Figure 3a shows the magnitude of the CL-adjustment, K_{Jm}- K_{Jc}, applied for the 7dpa irradiated toughness data versus K_{Jm} in red diamonds along with corresponding results for unirradiated and low dose irradiated specimens in black open square and blue circles, respectively, as previously reported [5]. The adjustments follow a similar trend. The 7dpa data adjustments are only slightly larger than the average trend for the previous cases, shown in solid green line. Indeed larger differences might be expected in view of the lower strain hardening, smaller σ^*/σ_y ratio as well as the thinner specimen. Note, the adjustment would have been much more in the 7dpa case if a higher toughness had been measured as would occur higher test temperature. Note the proportionality between K_{Jm} and the constraint adjustment means that any larger scatter in the measured toughness is highly compressed in CL-adjusted toughness.

The reason for this behavior and important implications are illustrated in Figure 3b showing the variation in the normalized stress area for σ^*/σ_y= 2 as a function of $(J/b\sigma_y)^2$ in both the 7 dpa and 0.12 dpa irradiated specimens. In the latter case, the curve approaches a constant slope, which means that as the measured K_{Jm} increases it is adjusted by an almost equal amount back to only a slightly higher K_{Jc}. This is

to some extent an artifact of the procedure and means that actual variations in K_{Jc}, which could be measured in larger specimens, cannot be detected in small specimens beyond a $J/b\sigma_y$ deformation limit. The limited toughness measurement capacity is even more severe for 7dpa specimen where the stress area reaches saturation level at $(J/b\sigma_y)^2 \approx 0.001$ that corresponds to $K_{Jm} \approx 110$ MPa$\sqrt{m}$ for this specimen size and geometry. The saturation is largely due to the large strain hardening loss in the more highly irradiated condition. Adjusted 1T-toughness would never be more than $\approx$ 40 MPa$\sqrt{m}$ in the 7 dpa irradiation case, or the specimen will more likely experience ductile tearing or plastic collapse as alternatives to mode cleavage. In fact some tests showed data clearly separated into two extreme cases – ones showing very low toughness and the others with no cleavage [25,26]. Such testing limit of small size specimens must be recognized, especially for materials with low strain hardening capacity.

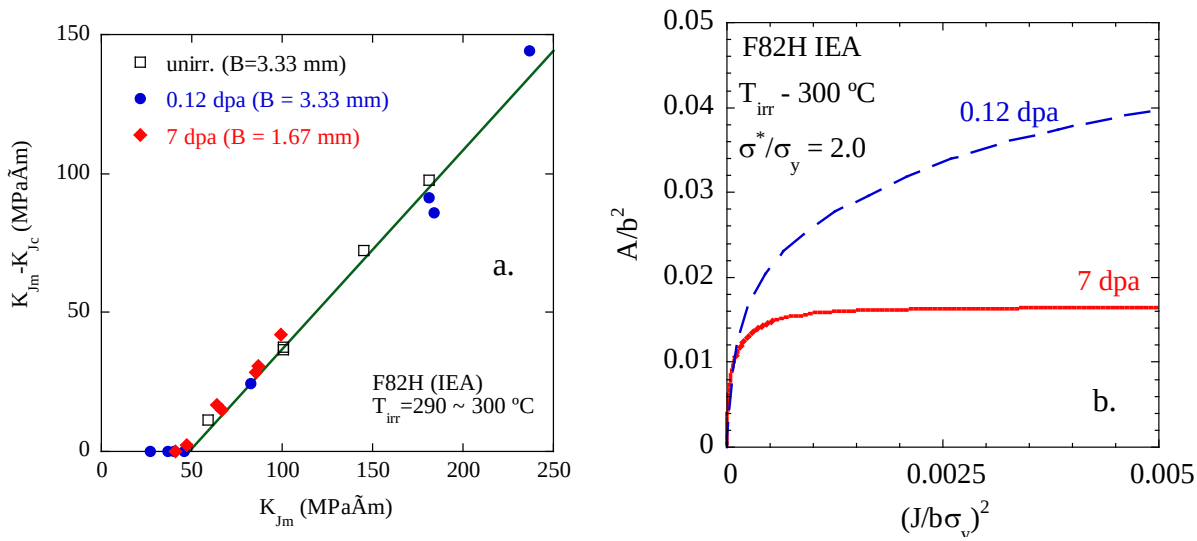

Figure 3 a) magnitude of the constraint loss adjustment as a function of measured toughness and b) normalized stressed area versus normalized loading relations in F82H irradiated to 0.12 and 7 dpa at $\approx$ 300 ºC.

Conclusions

A combined constraint loss and statistical size adjustment procedure was applied to fracture toughness data for small pre-cracked bend bar specimens (W = 3.33, B = 1.67 and L = 18 mm) for the IEA heat of F82H irradiated to $\approx$ 7 dpa at $\approx$ 300ºC in HFIR. The cleavage transition MC reference temperature shifts, based on the measured toughness, $K_{Jm}(T)$, data (ΔT_m) as well as reference temperature shifts (ΔT_o) found after size-adjusting the $K_{Jm}(T)$ data yielded $\Delta T_{m/o} \approx$ 148 and 205 ºC, respectively. The $C_o = \Delta T_o/\Delta\sigma_y$ = 0.51 is in good agreement with but falls slightly below corresponding data in the literature. A more universal measure of shifts related to irradiation hardening is based on the low stress change and gives the $C_o = \Delta T_o/\Delta\langle\sigma_{fl}\rangle$ = 0.68 in excellent agreement with model predictions. The FE analyses also showed that crack tip stressed area saturates at much lower deformation level in the F82H IEA after 7 dpa irradiation, primarily due to loss of strain hardening. These results demonstrate that there are upper limits on K_{Jc} values that can be measured with small specimens that are further decreases in highly irradiated steels that suffer severe loss of strain hardening capacity.

Acknowledgements:

Experimental data used in this study were obtained under the collaboration with Oak Ridge National Laboratory, Pacific Northwest National Laboratory and Japan Atomic Energy Agency. The authors are grateful to Drs. Steve Zinkle, Roger Stoller, Shiro Jitsukawa, Hiroyasu Tanigawa and other researchers involved in the US-JAEA collaboration. The research performed at University of California, Santa Barbara was supported by the US Department of Energy, Office of Fusion Science Grant #DE-FG03-94ER54275 and US Department of Energy, NERI Grant #DE-FG07-05ID14663.

References

[1] G. R. Odette, T. Yamamoto, H.J. Rathbun, M.Y. He, M.L. Hribernik, J.W. Rensman, *J. Nucl. Mater.* **323** (2003) 313.

[2] K. Wallin, A. Laukkanen, S. Tahtinen, *Small Specimen Test Techniques 4*, ASTM STP 1418 (2002) 33.

[3] G. R. Odette, T. Yamamoto, H. Kishimoto, M. Sokolov, P. Spätig, W. J. Yang, J. -W. Rensman and G. E. Lucas, *J. Nucl. Mater.* **329-333** (2004) 1243

[4] ASTM E 1921-09, "Standard Test Method for Determination of Reference Temperature, To, for Ferritic Steels in the Transition Range," ASTM, 2009.

[5] T. Yamamoto, G.R. Odette, D. Gragg, H. Kurishita, H. Matsui, W.J. Yang, M. Narui, M. Yamazaki, *J. Nucl. Mater.* **367-370** (2007) 593.

[6] T. Yamamoto, G. R. Odette, H. Kishimoto, J-W. Rensman, P. Miao, *J. Nucl. Mate*r. **356** (2006) 27,

[7] R. Kasada, T. Morimura, A. Hasegawa, A. Kimura, *J. Nucl. Mater.* 299 (2001) 83.

[8] Y. Dai, Z. Tong, L. Peng, G.R. Odette, T. Yamamoto, *this conference.*

[9] H.J. Rathbun, G.R. Odette, M.Y. He, T. Yamamoto, *Eng. Fracture Mechanics*, **73** (2006) 2723.

[10] G.R. Odette, M.Y. He, T. Yamamoto, *J. Nucl. Mater.* **367-370** (2007) 561.

[11] H.J. Rathbun, G.R. Odette, T. Yamamoto, M.Y. He, G.E. Lucas, *Eng. Fracture Mechanics*, **73** (2006) 134.

[12] M. A. Sokolov and R. K. Nanstad, *Effects of Irradiation on Materials-18th International Symposium,* ASTM STP 1325 (1999) 167.

[13] G. R. Odette, H. J. Rathbun, J. W. Rensman and F. P. van den Broek, *J, Nucl. Mater.* **307-311** (2002) 1624.

[14] M.A. Sokolov, G.R. Odette, T. Yamamoto, H. Tanigawa, H. Okubo, this conference.

[15] M.Y. He, G.R. Odette, T. Yamamoto, D. Klingensmith, *J. Nucl. Mater.* **367-370** (2007) 556.

[16] T. Yamamoto, Y. Dai, G.R. Odette, M. Salston, P. Miao, *Trans. American Nuclear Society,* 98 (2008) 1111.

[17] T. Hirose, H. Okubo, H. Tanigawa, M. Ando, M.A. Sokolov, R.E. Stoller, this conference.

[18] G.R. Odette, M.Y. He, E.G. Donahue, G.E. Lucas, ASTM STP 1418 (2002) 221.

[19] G.R. Odette, M. He, D. Gragg, D. Klingensmith, G.E. Lucas, *J. Nucl. Mater.*, **307-311** (2002) 1643

[20] M.L. Hribernik, G.R. Odette, T. Yamamoto, to be published.

[21] G. R. Odette, J. Nucl. Mater., **212-215** (1994) 45.

[22] T.L. Anderson, *Fracture Mechanics: Fundamentals and Applications,* Third Ed., CRC Press, Boca Raton, Florida, 2005.

[23] P. Spatig, "Small-scale fracture mechanics – modeling of brittle to ductile transition behaviors using appropriate theories. Formation of rules for transferability to standards and fusion components," TTW2-TTMS-005b, CPPI, Switzerland (2005)

[24] M.A. Sokolov, R.L. Klueh, G.R. Odette, K. Shiba and H. Tanigawa, ASTM STP 1447 (2004) 408

[25] P. Spatig, G. R. Odette, G. E. Lucas, *J. Nuc. Mater.* **275** (1999) 324

[26] J. W. Rensman, personal communication.